Supplementary Information

Ligand-Decoration Determines the Translational and Rotational Dynamics of Nanoparticles on a Lipid Bilayer Membrane

Zhihong Zhang,[a] Wendong Ma,[a] Kejie He,[a] Bing Yuan[a,*] and Kai Yang [a,*]

[a] Center for Soft Condensed Matter Physics and Interdisciplinary Research & School of Physical Science and Technology, Soochow University, Suzhou, 215006, P. R. China. E-mail: yuanbing@suda.edu.cn, yangkai@suda.edu.cn

Table S1. Simulated Systems and parameters.

System	NP diameter (nm)	Simulation length (μs)	Simulation times
NP + 512 DLPC	3	10	5
NP-8P + 512 DLPC	3	10	5
NP-16P + 512 DLPC	3	10	5
NP-8M + 512 DLPC	3	10	5
NP-16M + 512 DLPC	3	10	5
NP-8PM+512 DLPC	3	10	5

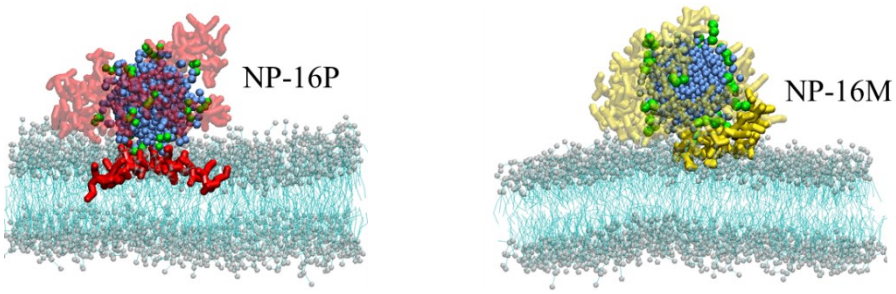

Figure S1. Typical snapshots during the membrane interactions of a NP-16P or -16M.

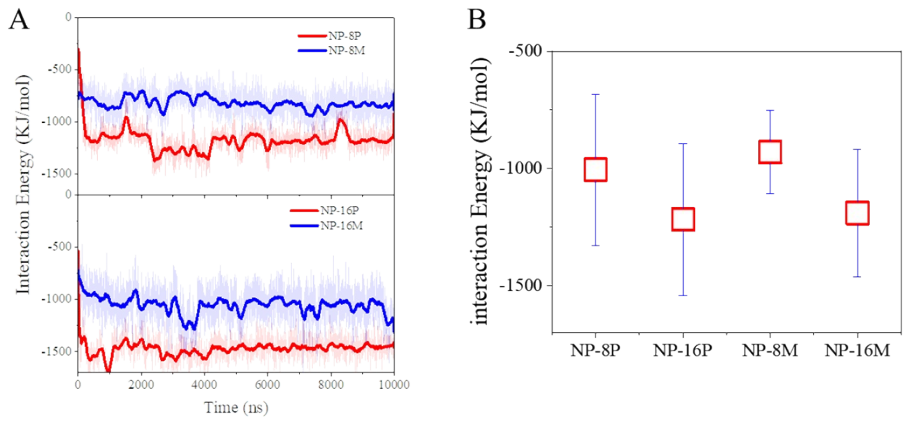

Figure S2. Interaction energy between the inserted peptides on the NP surface and the membrane. (A) Evolution of the interaction energy at varying ligand density. (B) Averaged membrane interaction energy of the inserted peptides in different NP systems. All results are obtained based on 5 independent runs.

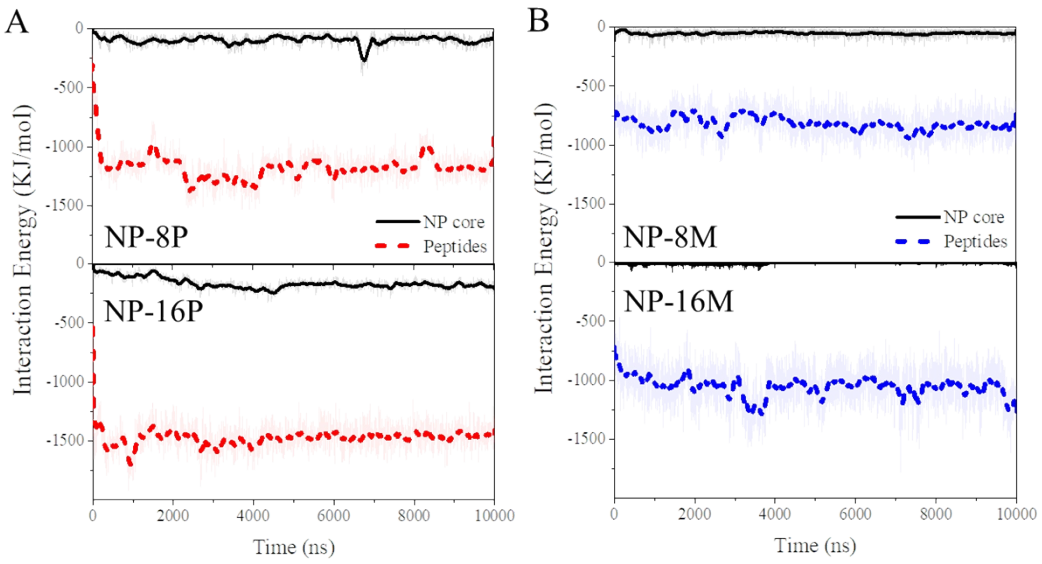

Figure S3. Comparison of the interaction energy between the NP core-membrane and coated peptide-membrane.

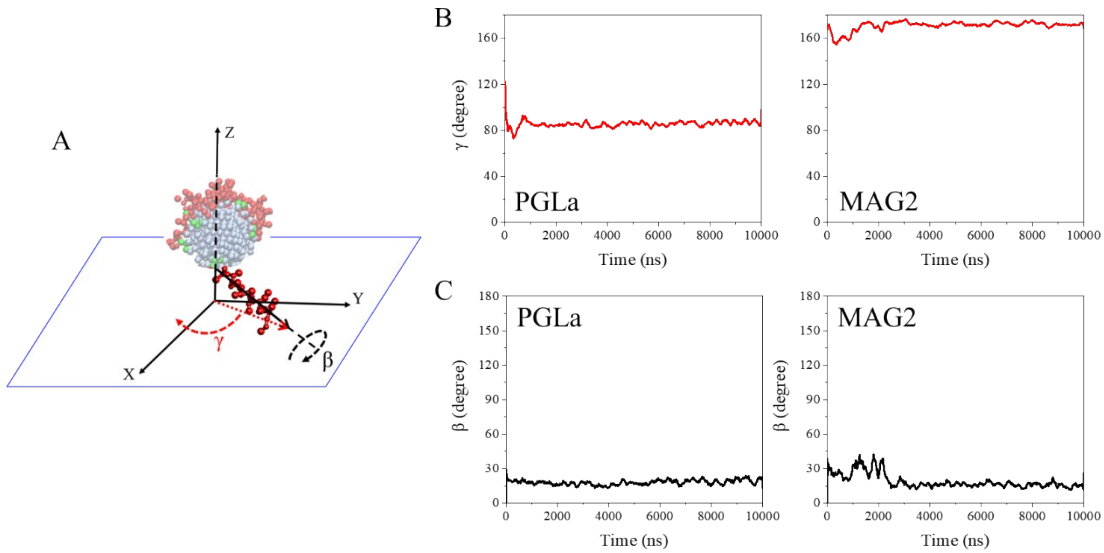

Figure S4 Possible rotation of the membrane-bound peptide. (A) Sketches of the two angles, γ and β, used to describe the configuration of the membrane-bound peptide in the membrane. (B, C) Time evolution of γ or β of the inserted PGLa and MAG2.

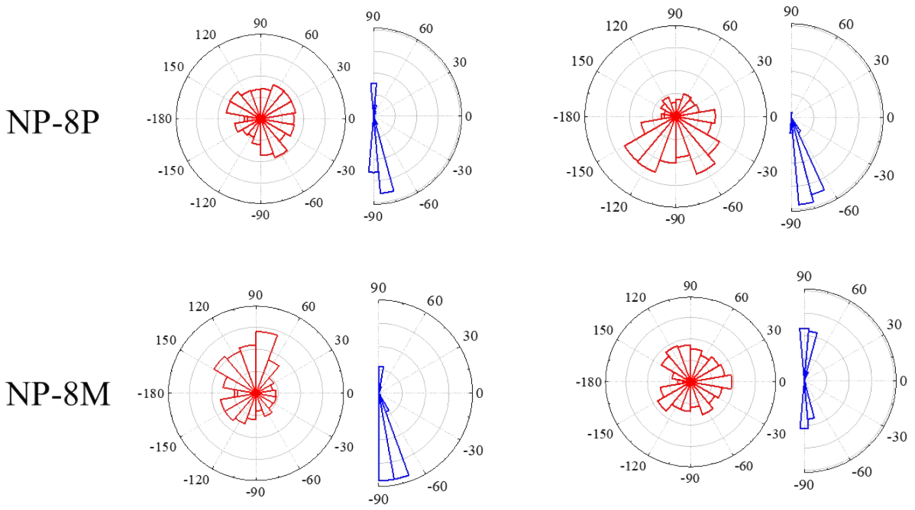

Figure S5. More distributions of the azimuthal angle φ and polar angle θ of different membrane-bound NPs.

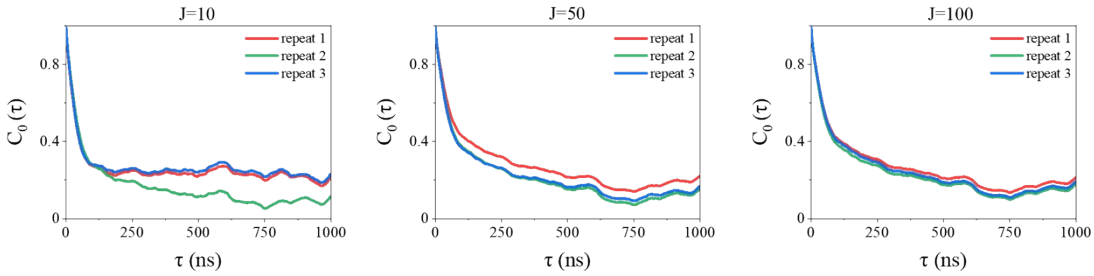

Figure S6. Influence of the vector number (J) on the calculation of C_0.

Note: The NP rotation is quantitatively characterized by the correlation function $C_0 = \frac{1}{T-\tau}\int_0^{T-\tau} \langle P_2(n_j(t+\tau)\cdot n_j(t))\rangle_J dt$. Here, a number of vectors, n_j (j=1, 2, 3, …, J =100), which are the randomly distributed unit vectors with respect to the NP reference frame (see the inset of Fig. 4 in the main text), are chosen to fully characterize the NP orientation. It is found that, with a large vector number J (e.g., J=100), even when the vectors are chosen arbitrarily in repeated calculations, the calculated C_0 remains almost the same (Figure S6). This suggests a good description of the changes of NP orientation, as well as its rotation.

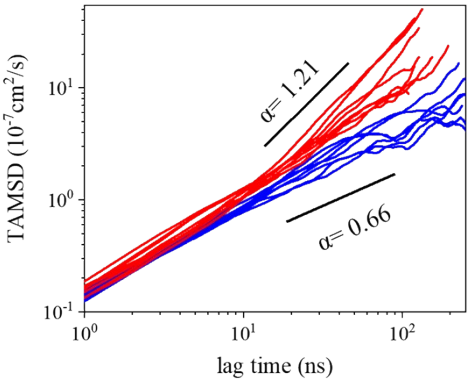

Figure S7. TAMSDs as a function of lag time on log-log scales of the hopping (red) and confined (blue) motions.

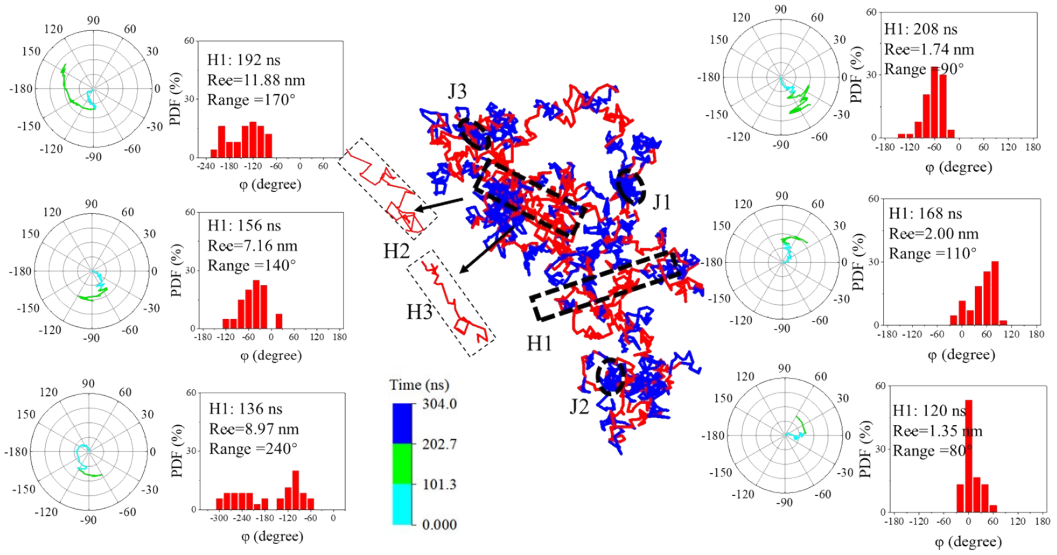

Figure S8. Another typical trajectory of NP-8P on the membrane surface. The hopping and jiggling stages are drawn in red and blue, respectively, and some of them are representatively marked with dashed box (hopping) or circle (jiggling). The evolution of φ in a certain stage and its corresponding PDF distribution are given.

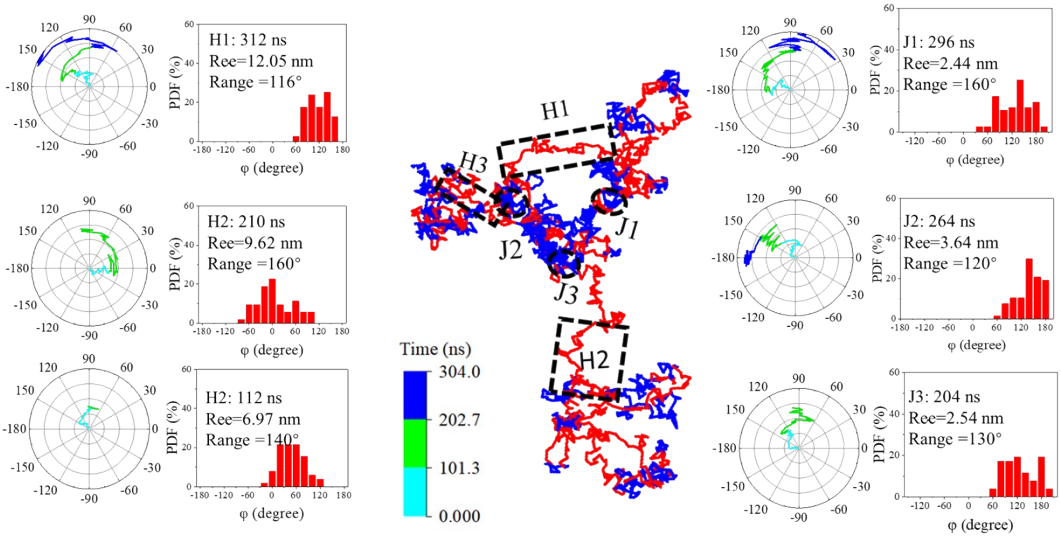

Figure S9. Another typical trajectory of NP-8M on the membrane surface. The hopping and jiggling stages are drawn in red and blue, respectively. Some typical stages at different time intervals are chosen (hopping: dashed box; jiggling: dashed circle). The evolution of φ in a certain stage and its corresponding PDF distribution are also given.

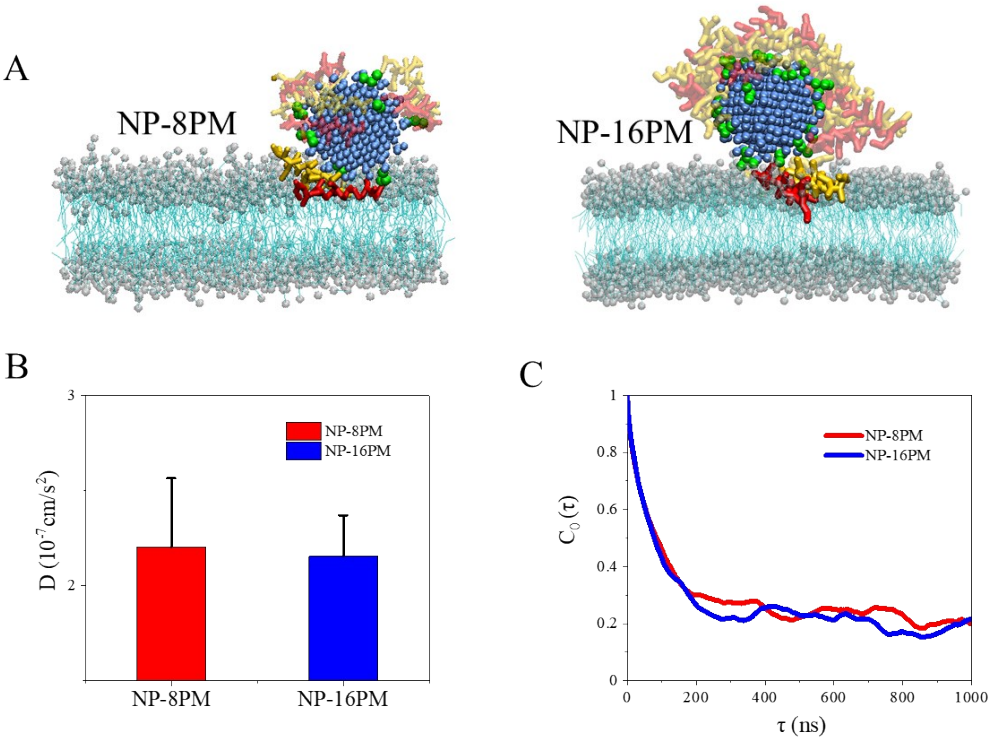

Figure S10 Dynamics of NP-8PM and NP-16PM on the membrane. (A) Typical snapshots showing the membrane-binding states of NP-8PM and NP-16PM. (B-C) Diffusion coefficient D and rotational correlation function C_0 of NP-8PM and NP-16PM.